

Baroclinic Energy Conversion across Topographically Rough Straits with Application to Luzon Strait

Sutanu Sarkar
University of California at San Diego
La Jolla, CA 92093
Tel: 858-534-824, Fax: 858-534-7599, sarkar@ucsd.edu

Award N00014-09-10287
<http://maeresearch.ucsd.edu/SARKAR/>

LONG-TERM GOALS

The goal of is to assess the relative contribution of local dissipation versus far-field radiation of internal waves generated by the barotropic tide flowing across topographically rough straits in the Western Pacific.

OBJECTIVES

- Perform large eddy simulation (LES) of a bottom boundary layer on rough topography to quantify near-bottom mixing as a function of slope angle, stratification strength and other parameters.
- Integrate the UCSD LES Model with the UNC Ocean Model in a joint effort with A. Scotti to cover a realistic range of spatial and temporal processes deemed important to the near-field mixing observed in the field experiment.

APPROACH

A non-hydrostatic model that numerically solves the unsteady, three-dimensional, primitive equations is used. Advanced models such as the dynamic mixed model and the dynamic eddy viscosity model are utilized to represent subgrid processes in the LES approach. A novel near-wall model has been developed so as to increase the Reynolds number of boundary flows to realistically large geophysical values.

WORK COMPLETED

During the first year of the grant, significant effort was expended in advancing the capabilities of the numerical solver. This has allowed us to contrast the boundary layer among the cases of subcritical, critical and supercritical slope.

Model problem

The near-bottom flow resulting from a current oscillating with the M_2 tidal period of 12.4 hrs. on an inclined surface, as illustrated in Fig 1, is simulated. The bottom is adiabatic while there is a background thermal stratification with constant buoyancy frequency, N_∞ . The flow is forced

Report Documentation Page

Form Approved
OMB No. 0704-0188

Public reporting burden for the collection of information is estimated to average 1 hour per response, including the time for reviewing instructions, searching existing data sources, gathering and maintaining the data needed, and completing and reviewing the collection of information. Send comments regarding this burden estimate or any other aspect of this collection of information, including suggestions for reducing this burden, to Washington Headquarters Services, Directorate for Information Operations and Reports, 1215 Jefferson Davis Highway, Suite 1204, Arlington VA 22202-4302. Respondents should be aware that notwithstanding any other provision of law, no person shall be subject to a penalty for failing to comply with a collection of information if it does not display a currently valid OMB control number.

1. REPORT DATE 2009	2. REPORT TYPE	3. DATES COVERED 00-00-2009 to 00-00-2009			
4. TITLE AND SUBTITLE Baroclinic Energy Conversion across Topographically Rough Straits with Application to Luzon Strait		5a. CONTRACT NUMBER			
		5b. GRANT NUMBER			
		5c. PROGRAM ELEMENT NUMBER			
6. AUTHOR(S)		5d. PROJECT NUMBER			
		5e. TASK NUMBER			
		5f. WORK UNIT NUMBER			
7. PERFORMING ORGANIZATION NAME(S) AND ADDRESS(ES) University of California at San Diego, La Jolla, CA, 92093		8. PERFORMING ORGANIZATION REPORT NUMBER			
9. SPONSORING/MONITORING AGENCY NAME(S) AND ADDRESS(ES)		10. SPONSOR/MONITOR'S ACRONYM(S)			
		11. SPONSOR/MONITOR'S REPORT NUMBER(S)			
12. DISTRIBUTION/AVAILABILITY STATEMENT Approved for public release; distribution unlimited					
13. SUPPLEMENTARY NOTES					
14. ABSTRACT					
15. SUBJECT TERMS					
16. SECURITY CLASSIFICATION OF:			17. LIMITATION OF ABSTRACT Same as Report (SAR)	18. NUMBER OF PAGES 6	19a. NAME OF RESPONSIBLE PERSON
a. REPORT unclassified	b. ABSTRACT unclassified	c. THIS PAGE unclassified			

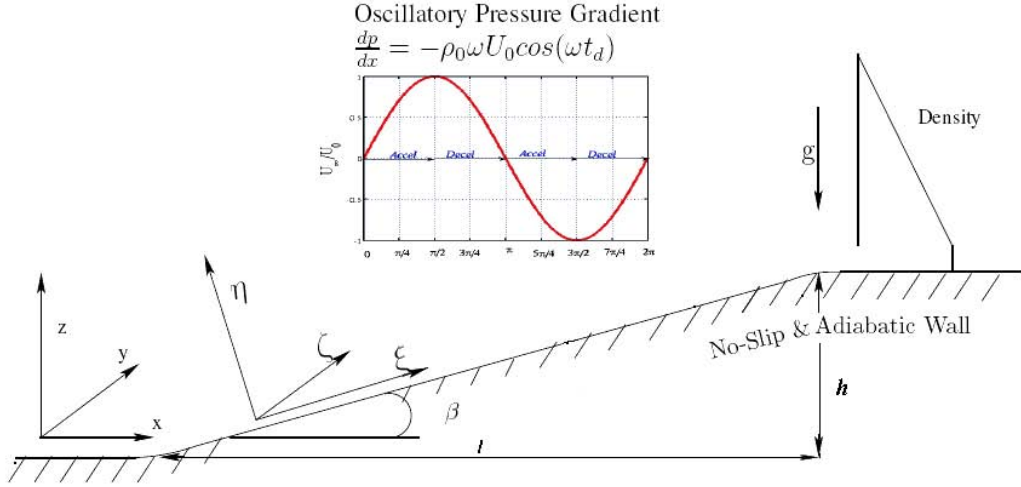


Figure 1: Schematic of the problem

by an imposed pressure gradient along the horizontal direction resulting in a barotropic current of $U_0 \sin(\Omega t_d)$ in the background. Here coordinates x , y and z denote the horizontal streamwise, horizontal spanwise and vertical directions, and u , v and w denote the corresponding velocity components. The coordinates ξ , ζ and η correspond to the curvilinear grid that conforms to the bottom topography.

The dimensional parameters that set the flow and the thermal field are as follows: the freestream velocity amplitude U_0 , tidal frequency Ω , background density gradient $d\rho_d^b/dz_d|_{\infty}$, and the fluid properties: molecular viscosity ν , thermal diffusivity κ , and density ρ . The parameters that set the geometry are as follows: slope angle, β , the slope length in x -direction, and the nominal water depth, H . The Coriolis parameter is taken to be $f = 0$. There are a number of important nondimensional parameters that govern the flow over the slope. The values of tidal excursion parameter, $Ex = U_0/(\omega l)$ and the ratio of topography height to the water depth are taken to be small values to correspond to tidal flow over a slope in deep water. Moderate values of N are considered. As a first step, the Reynolds number is small corresponding to unsteady transitional flow rather than full-blown turbulence at the bottom.

The angle θ that internal wave phase lines forced at the tidal frequency, Ω , makes with the horizontal is given by

$$\tan^2(\theta) = \frac{\Omega^2 - f^2}{N^2 - \Omega^2}. \quad (1)$$

The value of the slope criticality parameter, $\epsilon = \tan(\beta)/\tan(\theta)$ determines the slope response. Three cases have been simulated: subcritical $\epsilon = 0.5$, near critical $\epsilon \simeq 1$ and supercritical $\epsilon = 1.7$.

Numerical algorithm development

In the streamwise (x) direction, the spatial discretization has been changed from Fourier collocation and boundary conditions have been changed from periodic, in order to allow streamwise (x) development, key to the boundary flow on a slope. The spatial discretization corresponds to a staggered finite-difference grid in the x , z directions and Fourier collocation in the spanwise, y , direction. Spatial y -derivatives are computed in spectral space while those in the other two directions are computed using second-order finite difference. Time advancement is accomplished using a third-order Runge-Kutta method. The viscous derivatives are treated implicitly

using an alternating direction implicit (ADI) method for improved stability characteristics. The boundary conditions on the velocity are as follows: Inflow/outflow boundary conditions along with sponge regions, no-slip at the bottom boundary for the resolved, moderate-Reynolds number cases considered here, sponge region at the top boundary and periodic at the lateral, side boundaries. An equation for the deviation from the background density is numerically solved with boundary conditions correspond to sponge regions, periodicity in the lateral direction or prescribed slope-normal gradient at the bottom.

In order to handle bottom topography, the Navier-Stokes equations have been recast in generalized curvilinear coordinates. The governing equations are transformed to a strong conservation law. A curvilinear grid-generation module has also been added to design a grid that conforms to the bottom boundary. The grid is clustered in the near-bottom region.

The Navier-Stokes equations are solved using a fractional step method. The pressure correction satisfies a Poisson equation which, in the present case, takes the form of a two-dimensional Helmholtz equation. A multigrid solver is employed with the following characteristics: incomplete L-U decomposition as the smoother, weighted 9-point prolongation and restriction, and sawtooth cycling, that is, smoothing only during grid transfers that occur during the prolongation phase of the multigrid cycle.

RESULTS

Near-critical case, $\epsilon \simeq 1$

Phase lines of the internal waves at the fundamental frequency, Ω , of the M_2 tide are parallel to the slope when $\epsilon \simeq 1$ leading to the phenomenon of resonant generation. A tidal beam emanates to the right as shown in Fig. 2. Owing to the baroclinic internal wave component, the velocity in the boundary layer is amplified relative to the peak barotropic value so that the kinetic energy is as large as ten times larger than the background barotropic value.

The density field has a response that is asymmetric between upflow and downflow as shown in Figure 3 for the near-critical case. During upflow, there is positive vertical strain and the stratification decreases while during downflow the stratification increases. The response of the disturbance kinetic energy to such a periodic modulation of the stratification is currently under investigation.

Supercritical case, $\epsilon = 1.7$

Internal waves are generated at the upper portion of the slope where the topography transitions from supercritical slope to horizontal. Similar to the case with $\epsilon \simeq 1$, there is a significant tidal beam associated with the near-critical extent of the slope near the top as shown in Figure 4. However, an important difference is the presence of energetic beams at steeper angles. The power spectrum of the streamwise velocity in Figure 5 shows clear evidence of harmonics, $n\Omega$ of the tidal frequency. The kinetic energy beams with steeper angles correspond to these harmonics.

IMPACT/APPLICATIONS

Three-dimensional, highly-resolved simulations of the bottom boundary layer under a barotropic tide on a slope have been performed. The difference between subcritical, critical and supercritical slopes with respect to the mean velocity and the internal wave field has been highlighted. The impact of slope criticality on turbulence and dissipation rates will be obtained during the second year.

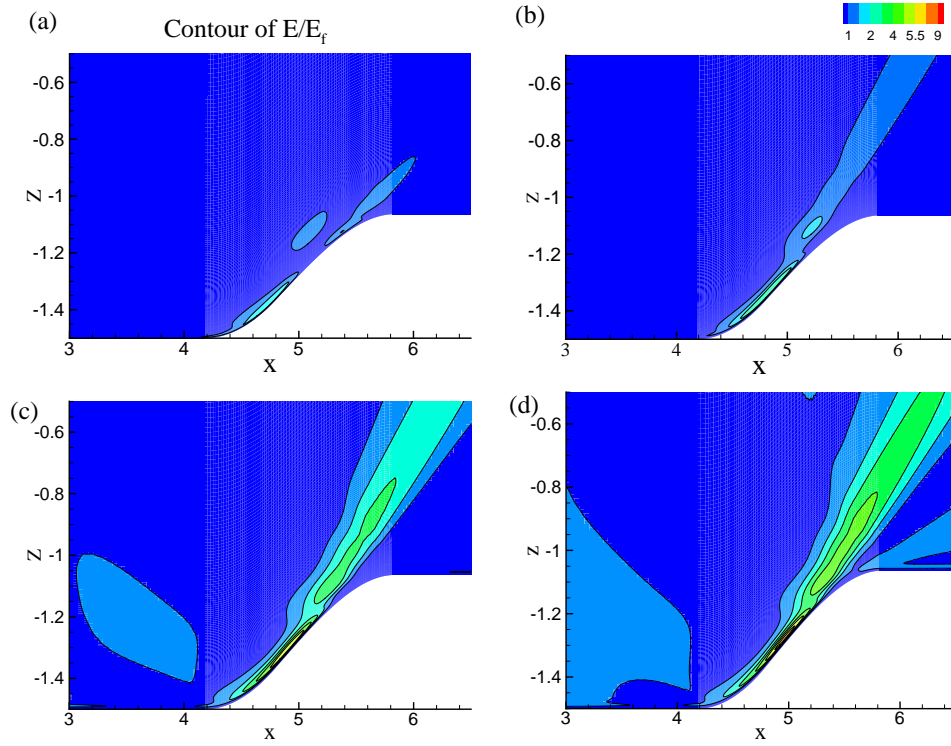


Figure 2: Resonant generation in the near-critical case, $\epsilon \simeq 1$ shown by contours of E/E_f , where E is the kinetic energy whose freestream value is $E_f = 0.5U_0^2$. The tidal phase is denoted by ϕ and the peak slope-parallel velocity is U_p . The values of ϕ for (a), (b), (c) and (d) are $3\pi/4$, π (zero freestream velocity), $9\pi/8$ and $5\pi/4$, respectively, and corresponding values of peak velocity are $U_p/U_0 = 2.45, 2.83, 3.62$ and 3.01 , respectively.

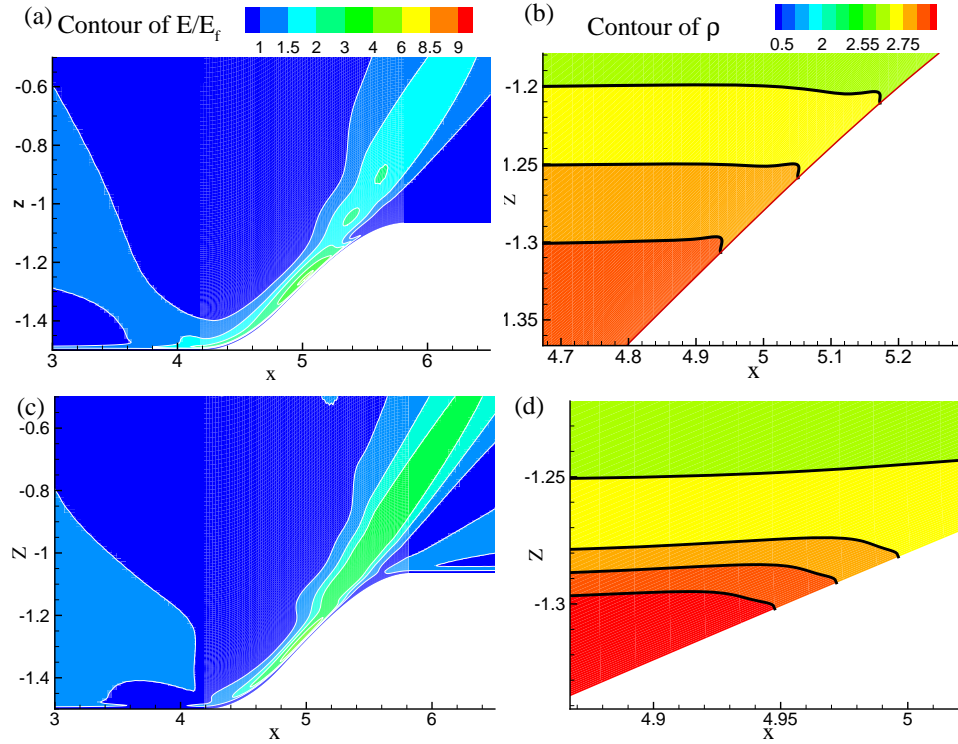


Figure 3: Top panel corresponds to a phase of $\pi/8$ where there is upflow with peak velocity $U_p/U_0 = 3.6$: (a) Kinetic energy contours, (b) Isopycnals. Bottom panel, phase of $9\pi/8$ corresponds to downflow with $U_p/U_0 = -3.62$: (a) Kinetic energy contours, (b) Isopycnals.

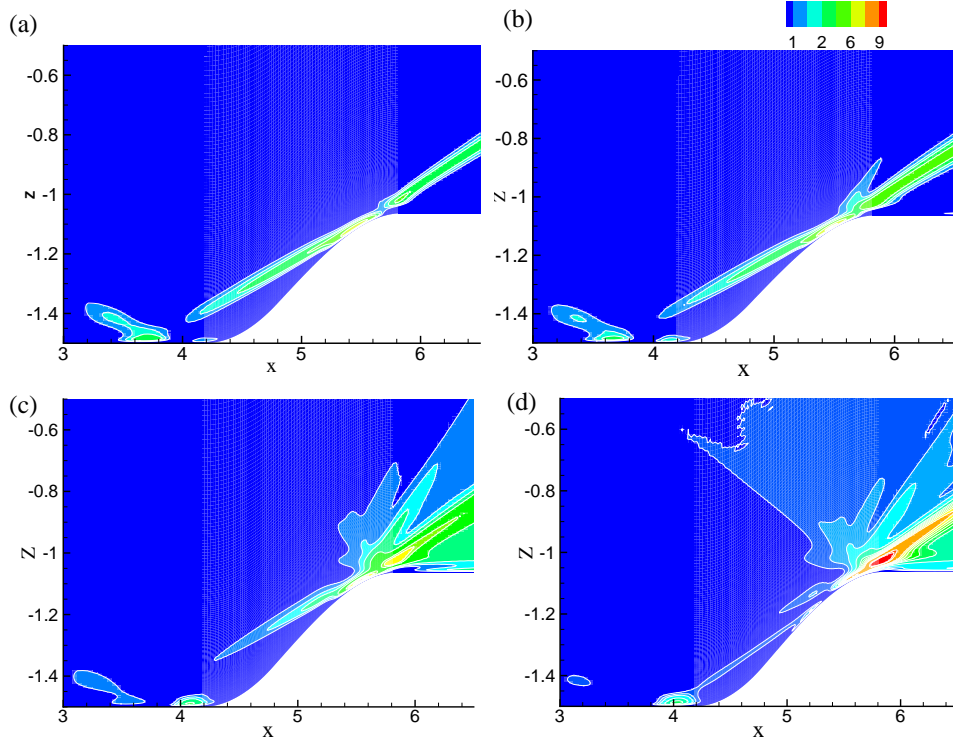


Figure 4: Generation in a supercritical case, $\epsilon = 1.7$. Contours of E/E_f , where $E_f = 0.5U_0^2$, are shown. The tidal phase is (a) $\phi = 3\pi/4$, (b) $\phi = \pi$, (c) $\phi = 5\pi/4$ and (d) $\phi = 3\pi/2$, respectively.

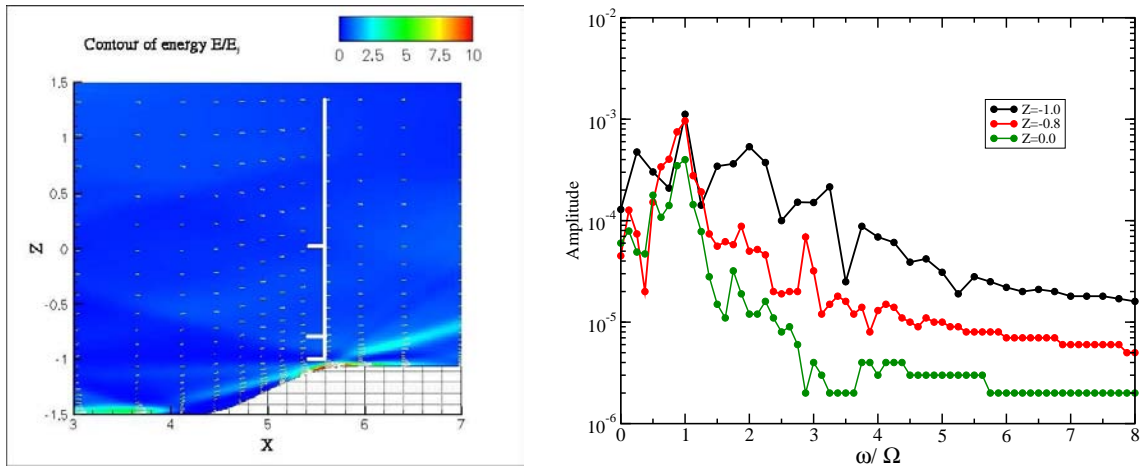


Figure 5: Power spectra of the streamwise velocity (semi log-scale) as a function of frequency in the case with $\epsilon = 1.7$ in (b). The corresponding spatial positions are shown by three small white horizontal lines in (a).